

# Investigating the parton shower model in PYTHIA8 with pp collision data at $\sqrt{s} = 13 \text{ TeV}$ \*

S. K. Kundu<sup>1†</sup>, T. Sarkar<sup>2‡</sup>, M. Maity<sup>3§</sup>

<sup>1,3</sup> Visva-Bharati University, Santiniketan, India

<sup>2</sup> National Central University (NCU), Taiwan.

## Abstract

Understanding the production of quarks and gluons in high energy collisions and their evolution is a very active area of investigation. Monte carlo event generator PYTHIA8 uses the parton shower model to simulate such collisions and is optimized using experimental observations. Recent measurements of event shape variables and differential jet cross-sections in pp collisions at  $\sqrt{s} = 13 \text{ TeV}$  at the Large Hadron Collider have been used to investigate further the parton shower model as used in PYTHIA8.

## 1 Introduction

Matrix element calculations with fixed order treatment is not sufficient to understand the production of quarks and gluons, collectively called partons, in high energy collisions or their evolution into jets of hadrons. Comparison with experimental results demand fully exclusive description of the final states based on the shower evolution and hadronization. Such methods are described through phenomenological models embedded in the shower Monte Carlo (MC) codes.

PYTHIA8 uses leading order(LO) calculations followed by ‘transverse momentum’ ( $p_{\perp}$ ) ordered parton shower[1] with  $p_{\perp}^2$  as evolution variable for the generation of  $2 \rightarrow n$  ( $n \geq 2$ ) final states by taking account initial (ISR) and final (FSR) state shower. Shower evolution for a parton like  $a \rightarrow bc$ , is based on the standard (LO) DGLAP splitting kernels and the branching probability expressed as:

$$d\mathcal{P}_a = \frac{dp_{\perp}^2}{p_{\perp}^2} \sum_{b,c} \frac{\alpha_s(p_{\perp}^2)}{2\pi} P_{a \rightarrow bc}(z) dz \quad (1.1)$$

where  $P_{a \rightarrow bc}$  is the DGLAP splitting function and  $p_{\perp}^2$  represents the scale of the branching;  $z$  represents the sharing of  $p_{\perp}$  of  $a$  between the two daughters, with  $b$  taking a fraction  $z$  and  $c$  the rest,  $1 - z$ . Here the summation goes over all allowed branchings, e.g.  $q \rightarrow qg$  and  $q \rightarrow q\gamma$  and etc. Now, the divergence at  $p_{\perp}^2 \rightarrow 0$  is taken care of by introducing a

---

\*Presented at XXIV DAE-BRNS High Energy Physics Symposium

<sup>†</sup>sumankundu.rs@visva-bharati.ac.in

<sup>‡</sup>tanmay.sarkar@cern.ch

<sup>§</sup>manas.maity@visva-bharati.ac.in

PYTHIA8 Parameters set	Monash values	Sampling range	Optimized values
SpaceShower:alphaSvalue	0.1365	0.1092 – 0.1638	$0.11409^{+0.00078}_{-0.00073}$
TimeShower:alphaSvalue	0.1365	0.1092 – 0.1638	$0.15052^{+0.00077}_{-0.00076}$
SpaceShower:PTmaxFudge	1.0	0.6 – 1.4	$0.9323^{+0.0065}_{-0.0064}$

Table 1: Optimized result of three parameters of PYTHIA8 is shown along with their default values in the Monash tune and the sampling range.

term  $\mathcal{P}_a^{\text{no}}(p_{\perp\text{max}}^2, p_{\perp\text{evol}}^2)$  known as *Sudakov form factor* [2]. This Sudakov factor ensures that there will be no emission between scale  $p_{\perp\text{max}}^2$  to a given  $p_{\perp\text{evol}}^2$ .

Considering lightcone kinematics, evolution variables  $p_{\perp\text{evol}}^2$  for  $a \rightarrow bc$  at virtuality scale  $Q^2$  for space-like branching (ISR) and time-like branching (FSR) are given by  $(1 - z)Q^2$  and  $z(1 - z)Q^2$  respectively. Finally, equations 1.2 and 1.3 describe the evolutions for ISR and FSR respectively [1].

$$d\mathcal{P}_b = \frac{dp_{\perp\text{evol}}^2}{p_{\perp\text{evol}}^2} \frac{\alpha_s(p_{\perp\text{evol}}^2)}{2\pi} \frac{x' f_a(x', p_{\perp\text{evol}}^2)}{x f_a(x, p_{\perp\text{evol}}^2)} P_{a \rightarrow bc}(z) dz \mathcal{P}_b^{\text{no}}(x, p_{\perp\text{max}}^2, p_{\perp\text{evol}}^2) \quad (1.2)$$

$$d\mathcal{P}_a = \frac{dp_{\perp\text{evol}}^2}{p_{\perp\text{evol}}^2} \frac{\alpha_s(p_{\perp\text{evol}}^2)}{2\pi} P_{a \rightarrow bc}(z) dz \mathcal{P}_a^{\text{no}}(p_{\perp\text{max}}^2, p_{\perp\text{evol}}^2) \quad (1.3)$$

Currently both the running re-normalisation and factorisation shower scales, i.e. the scales at which  $\alpha_s$  and the PDFs are evaluated, are chosen to be  $p_{\perp\text{evol}}^2$  [3]. The general methodology of PYTHIA8 for ISR, FSR and MPI is to start from some maximum scale  $p_{\perp\text{max}}^2$  and evolve downward in energy towards next branching until the daughter partons reach some cut-off.

## 2 Optimizing the Parton Shower Model of PYTHIA8

CMS and ATLAS have done several tuning of PYTHIA8 around its Monash tune [4] for underlying event (UE), the strong coupling, and MPI related parameters [5, 6] [7]. In this study [8] Monash tune also used as default for PYTHIA v8.235 with NNPDF2.3 PDF (LO) set to optimize with four event shapes [9] measurement from CMS. These are - the complement of transverse thrust ( $\tau_{\perp}$ ), total jet mass ( $\rho_{\text{Tot}}$ ), total transverse jet mass ( $\rho_{\text{Tot}}^T$ ) and total jet broadening ( $B_T$ ).

Monash tune overestimates the multijet regions of these event shapes [9], Hence we examined ISR and FSR utilising the provision that PYTHIA8 allows the use of separate values of  $\alpha_s(M_Z)$  for the showering frameworks used for these. The maximum evolution scale involved in the showering is set to match the scale of the hard process itself. In PYTHIA8 it is set equal to the factorization scale, but allows its modification by multiplicative factors `SpaceShower:PTmaxFudge` for ISR and `TimeShower:PTmaxFudge` for FSR. The latter is seen not to have much effect on the ESVs, it is excluded from the optimization.

For each point in the parameter space, resulting distributions have been compared with data in terms of  $\chi^2/\text{NDF}$ . Then PROFESSOR v2.3.0 [10] along with RIVET v2.6 [11] has been used to optimize the complete set of ESV distributions from PYTHIA8 [9]. Post optimization, the new parameter set is checked [8] using other relevant results from the CMS [12] and ATLAS [13].

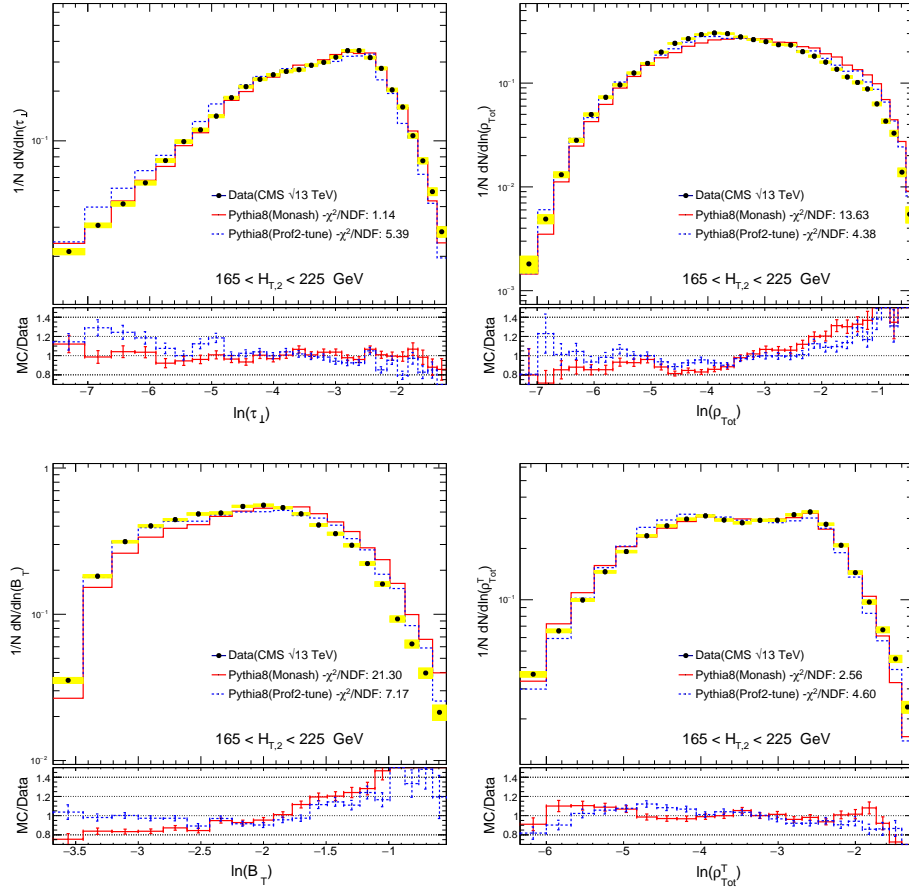


Figure 1: Predictions of the optimized parameter set is compared with CMS data and Monash tune for  $H_{T,2}$  range  $165 < H_{T,2} < 225$ . normalized distributions of the  $\tau_{\perp}$  (top left),  $\rho_{\text{Tot}}$  (top right),  $B_T$  (bottom left) and  $\rho_{\text{Tot}}^T$  (bottom right)

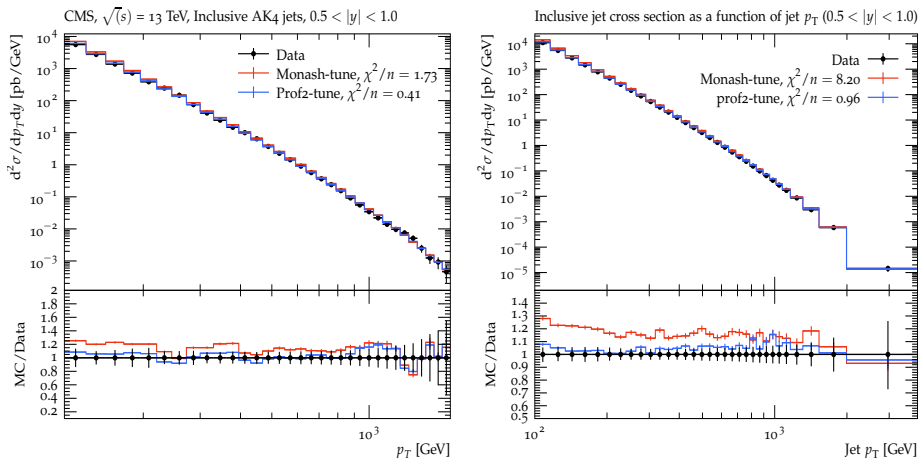


Figure 2: Normalized distributions of differential inclusive cross-section for anti- $k_T$  jets ( $R=0.4$ ) for CMS(left) and ATLAS(right) are compared with the predictions of PYTHIA8 with the optimized parameter set and Monash tune.

### 3 Validation of results

The optimized values of the three parameters (see, table 1) are used to calculate the ESVs. Agreement with data deteriorates slightly for  $\tau_{\perp}$  and  $\rho_{\text{Tot}}^T$  (figure 1) compared to the good agreement with the Monash tune. But, there is significant improvement in agreement with data for  $\rho_{\text{Tot}}$  and  $B_T$  (figure 1) compared to the Monash tune. Since  $\rho_{\text{Tot}}$  and  $B_T$  had a rather poor agreement between data and the Monash tune, overall this new set of parameters is better.

Inclusive jet cross-section measurements being sensitive to PDF of protons and  $\alpha_s$  are also compared with those optimized values. CMS [12] and ATLAS [13] studies with the 13 TeV data considered for this validation. The CMS measurements of inclusive cross-sections for anti- $k_T$  jets with  $R = 0.4, 0.7$ . Figures 2 show that the new parameter set improves the agreement between data and the Monash tune of Pythia8. Similar improvement is seen for the ATLAS measurement of anti- $k_T$  jets with  $R = 0.4$  (figure 2).

Since PYTHIA8 is widely used, its optimization is important. This study shows that certain aspects of the experimental observations can be better described with this optimized set of parameters.

### References

- [1] T. Sjostrand, P.Z. Skands, Eur. Phys. J. **C39**, 129 (2005). DOI 10.1140/epjc/s2004-02084-y
- [2] V.V. Sudakov, Sov. Phys. JETP **3**, 65 (1956). [Zh. Eksp. Teor. Fiz.30,87(1956)]
- [3] R. Corke, T. Sjostrand, JHEP **03**, 032 (2011). DOI 10.1007/JHEP03(2011)032
- [4] P. Skands, S. Carrazza, J. Rojo, Eur. Phys. J. C **74**, 3024 (2014). DOI 10.1140/epjc/s10052-014-3024-y
- [5] V. Khachatryan, et al., Eur. Phys. J. C **76**, 155 (2016). DOI 10.1140/epjc/s10052-016-3988-x
- [6] A.M. Sirunyan, et al., Eur. Phys. J. C **80**(1), 4 (2020). DOI 10.1140/epjc/s10052-019-7499-4
- [7] A. Buckley, in *Proceedings of the Sixth International Workshop on Multiple Partonic Interactions at the Large Hadron Collider*. CERN (CERN, Geneva, 2014), p. 29
- [8] S.K. Kundu, T. Sarkar, M. Maity, Int. J. Mod. Phys. A **34**(33), 1950219 (2019). DOI 10.1142/S0217751X19502191
- [9] A.M. Sirunyan, et al., JHEP **12**, 117 (2018). DOI 10.1007/JHEP12(2018)117
- [10] A. Buckley, H. Hoeth, H. Lacker, H. Schulz, J.E. von Seggern, Eur. Phys. J. **C65**, 331 (2010). DOI 10.1140/epjc/s10052-009-1196-7
- [11] A. Buckley, J. Butterworth, L. Lonnblad, D. Grellscheid, H. Hoeth, J. Monk, H. Schulz, F. Siegert, Comput. Phys. Commun. **184**, 2803 (2013). DOI 10.1016/j.cpc.2013.05.021
- [12] V. Khachatryan, et al., Eur. Phys. J. **C76**(8), 451 (2016). DOI 10.1140/epjc/s10052-016-4286-3
- [13] Measurement of inclusive-jet cross-sections in proton-proton collisions at  $\sqrt{s} = 13$  TeV centre-of-mass energy with the ATLAS detector. Tech. Rep. ATLAS-CONF-2016-092, CERN, Geneva (2016)